



OPTICS, IMAGE SCIENCE, AND VISION

Perfect matching of concave diffraction grating with continuously circular Bragg mirrors on SOI platform

YUZHENG MAO, 1,2 JINGPING ZHU, 1,2,* KE LI, 1,2 BINGZHENG DU, 1,2 AND XUN HOU1,2

¹Key Laboratory for Physical Electronics and Devices of the Ministry of Education, Xi'an Jiaotong University, Xi'an 710049, China ²Shaanxi Key Laboratory of Information Photonic Technique, Xi'an Jiaotong University, Xi'an 710049, China *Corresponding author: jpzhu@xjtu.edu.cn

Received 29 November 2018; revised 14 February 2019; accepted 21 February 2019; posted 22 February 2019 (Doc. ID 353081); published 22 March 2019

A concave diffraction grating (CDG), based on circular Bragg mirrors, was constructed on the 220 nm silicon-on-insulator (SOI) platform. This continuous and smooth dielectric mirror is employed to eliminate the extra scattering loss occurring at the connection with neighboring grating teeth. A perfect match between the Bragg condition and the grating condition was derived in order to determine the geometrical parameters of the grating profile, finite-difference time-domain (FDTD) simulation shows that the reflection of the designed Bragg mirror can be up to 99.7% over a broad bandwidth of 330 nm. And the grating with circular Bragg mirrors exhibits low insertion loss in a relatively high order of M = 5 with some unwanted diffraction orders suppressed, thus creating a large dispersion while keeping compact structure. © 2019 Optical Society of America

https://doi.org/10.1364/JOSAA.36.000641

1. INTRODUCTION

The optical wavelength division multiplexer (WDM) network has been the focus of extensive investigation recently, being driven by the explosive growth of the global internet traffic [1]. As a key constituent of the system, the demultiplexer could greatly expand the optical bandwidth and capacity by increasing the number of wavelength channels on an optical fiber [2,3]. The integrated planar waveguide devices [4], arrayed waveguide grating (AWG) [5], and concave diffraction grating (CDG) [6], are widely used to create a separation of wavelengths owing to their compactness and better stability. Both gratings have been realized in various material systems such as silica on silicon (SOS) [7,8], and silicon on insulator (SOI) [9,10]. AWGs are commonly based on a SOS platform, which offers advantages of low propagation losses and good coupling to the optical fiber with close cross-section size. However, the bending radius of the grating is high, and the chip size is large due to its lower index contrast. A reduction of size is available by introducing a high index contrast waveguide. The SOI is an attractive technological platform and appropriate candidate for photonic integration on-chip. This can be mainly attributed to the combination of high contrast and the compatibility with mature CMOS fabrication technology, allowing for the implementation of silicon photonics with small footprint and low cost [11]. However, the high contrast AWGs are very susceptible to phase errors that result from the slight width variation of the silicon waveguides, leading to increased crosstalk.

Compared to AWGs, CDGs demonstrated on the SOI present significant advantages of possible size reduction and less sensitive to the width variations, because they do not require a series of waveguides of different phase delay lines as in the case of an AWG [12], and only one free propagation region is needed [13]. The conventional CDG introduces a large Fresnel loss at the grating facets, thus resulting in a poor performance of the grating. A promising reported approach is the use of a multilayer dielectric reflector (Bragg mirror) replacing the deepetched grating tooth. A perfect Bragg mirror, i.e., the Bragg condition has been satisfied, can provide a high reflectivity approaching 100% and broad bandwidth. However, the Bragg CDG experiences other inherent loss related to the nature of the grating element. The energy incident on the grating is distributed into several diffraction orders, leading to less efficiency in a selected order. To reach an optimum in the given order, the blazing condition needs to be fulfilled. Some limitations may occur. If the match of blazing and Bragg condition is away from a perfect situation, a large number of Bragg periods is required to obtain a high reflection, and the designed wavelength band may shift with a narrower stopband [14].

In this Letter, a diffraction grating with circular Bragg mirrors based on Rowland mounting is designed on the SOI platform. Utilizing these continuous and smooth dielectric stripes, the scattering loss at the edge connecting adjacent facets can be neglected. The reflection condition of the Bragg mirror is determined by one-dimensional photonic crystal (1D PC)

bandgap theory [15,16]. With a perfect matching between the grating condition and Bragg condition, the CDG shows a high efficiency with broad bandwidth at an accurate designed wavelength. Most light beams get diffracted into a high order to create considerable linear dispersion. The numerical simulation results and analysis are also presented.

2. CIRCULAR BRAGG MIRROR-BASED GRATING

An integrated diffraction grating disperses the light coming from the source into different angles, so that a further component is required to bring the diffracted light into focus. A curved grating based on classical Rowland mounting is adopted here, which itself could perform the task of both dispersing and focusing the light into the outputs, as shown in Fig. 1(a).

The input and outputs are placed along a circle of radius R_{rc} (the Rowland circle). The grating teeth sit on a grating circle with a radius of curvature of $2R_{rc}$ which is tangent to the Rowland circle at the grating pole. The conventional configuration is a grating etched vertically into the slab waveguide, and metallized laterally, which presents an inherent absorption loss and requires extreme fabrication techniques. Classical Rowland-based Bragg CDG is implemented by simply replacing each single deep etched grating tooth with a Bragg reflector [17], which does not allow for a continuity of Bragg layers between successive facets, as shown in Fig. 1(b). It may introduce an extra transmission loss that occurs at the junction of the two adjacent facets. In Fig. 1(c), Bragg reflectors with straight dielectric strips are adopted to create continuous grating teeth for the CDG [18]. However, there has been a mismatch in the neighboring teeth because the grating teeth are curved along the grating circle for Rowland configuration, leading to an additional scattering loss and slight deviation of the grating period.

The solution proposed here is to use continuously circular Bragg mirrors to provide high reflection, shown in Fig. 2. Bragg mirrors made of circular dielectric stripes are curvedly constructed along a series of concentric arrangement circles whose center is point B (the crossing point of the Rowland circle and normal to the blazing tooth at the grating pole). The radius difference of the two adjacent circles equals the Bragg period d,

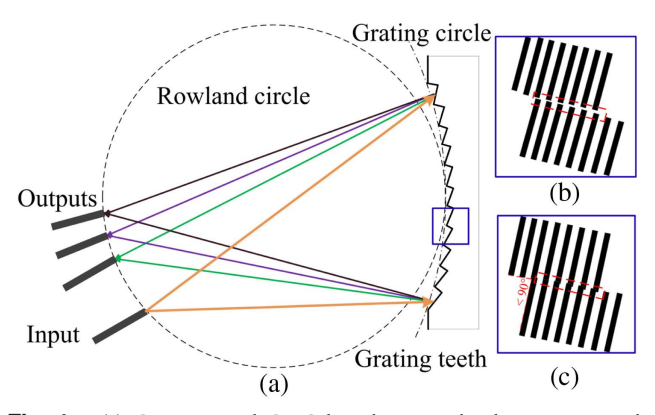


Fig. 1. (a) Conventional CDG based on Rowland mounting with deep etched grating teeth, (b) classical structure by replacing each tooth with a Bragg reflector, (c) curved grating with continuously straight dielectric strips reflectors.

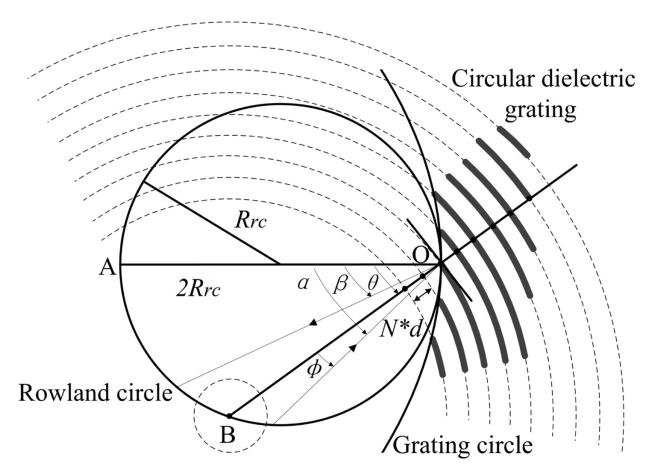


Fig. 2. Schematic layout and design geometrical parameters of a Rowland based concave diffraction grating with continuous circular Bragg mirrors.

thus keeping a parallelism and equidistance between the periodic elements all over the grating structure. In this way, a curved diffraction grating with continuously smooth Bragg mirrors is designed. And the problems associated with the edges between the neighboring facets are significantly suppressed. If the radius of the Rowland circle is large enough, the grating with circular Bragg mirrors tends to be a flat grating, and the grating period is respected.

3. DESIGN CONDITION

To interface constructively from the grating component, a perfect matching of diffraction grating condition and Bragg condition needs to be satisfied. The diffraction grating considered here consists of two different media, shown in Fig. 3.

 d_1 and d_2 are the width of the alternating strips with indices n_1 and n_2 , respectively, for the perspective layers, which creates a basic period d ($d = d_1 + d_2$) of the Bragg mirrors allowing the reflection of light. The grating facets are tilted at an angle θ to provide a blazing effect. N is the number of Bragg periods per grating period a. In the right triangle EPQ:

$$a = \frac{Nd}{\sin \theta}.$$
 (1)

 α and β are the incident and diffracted angles normal to the grating, respectively, as well as the incident angle ϕ on the

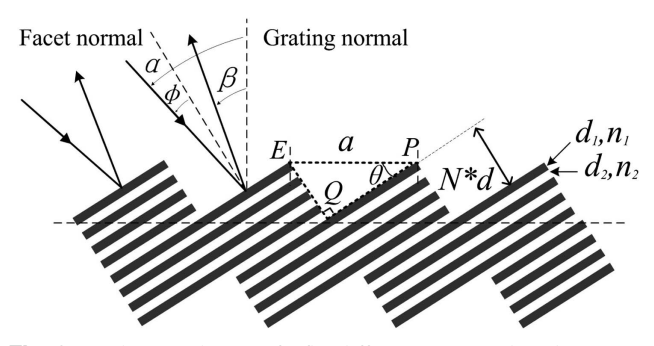


Fig. 3. Schematic layout of a flat diffraction grating based on Bragg mirrors.

Bragg facets. The diffraction condition, the difference in optical path by the adjacent grating teeth, has to be fulfilled,

$$M\lambda = n_{\text{eff}} a(\sin \alpha + \sin \beta),$$
 (2)

where M is the diffraction order, $n_{\rm eff}$ is the effective index of the slab mode in the free propagation region (FPR), and λ is the wavelength in a vacuum. To provide a maximum efficiency, the blazing condition needs to be satisfied, i.e., the angle of diffraction with respect to the facet normal is equal to the angle of reflection from the facet,

$$\theta - \beta = \phi. \tag{3}$$

From the grating geometry, we have

$$\alpha - \phi = \theta. \tag{4}$$

The following condition can be derived from the integration of Eq. (3) with Eq. (4),

$$\alpha + \beta = 2\theta, \qquad \alpha - \beta = 2\phi.$$
 (5)

With the above equation satisfied, the light beam will be diffracted constructively into a certain direction.

Up to this point, only the diffraction condition has been considered, and the reflection of Bragg mirror has also a profound impact on the performance of the grating. A Bragg mirror made of periodic dielectric layers can be analyzed by 1D PC bandgap theory. The propagation characteristics of light waves in such a structure are related to a unitary 2 × 2 translation matrix. h_1 is defined as the width ratio of the first dielectric layer, $h_1 = d_1/d$. It is convenient to display the band structure of the Bragg mirror by projecting the Block wave number (K) function $\omega(K, h_1)$ onto the $\omega - h_1$ plane [19]. With a given incident angle ϕ and index contrast, the projected band structure can be determined, as shown in Fig. 4. The solid black lines present the photonic bandgap edge of the Bragg mirror, where K is equal to zero. The white spaces are regions of propagating states (K is strictly real), whereas the gray areas represent regions exiting photonic bandgaps (K is imaginary).

With a proper width ratio h_1 selected, the light wave at a frequency of $\omega = \varpi \cdot 2\pi c/d$ within the gray area can be

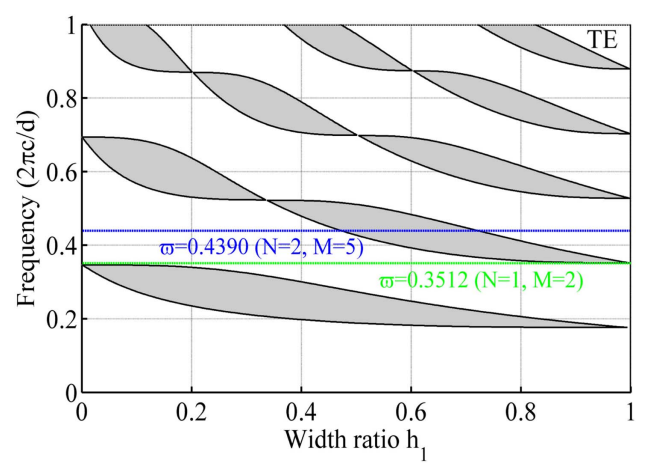


Fig. 4. Projected band structure of the Bragg mirror with an incident angel $\phi = 2^{\circ}$, refraction indices $n_1 = 2.848$ and $n_2 = 1.444$ for TE mode. Propagating states, white; evanescent states, gray.

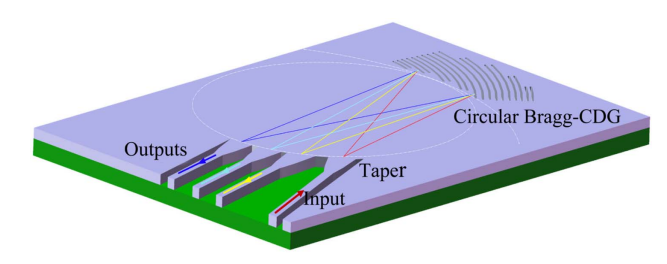


Fig. 5. Configuration layout of the circular Bragg mirror diffraction grating and access waveguides with parabolic tapers.

reflected efficiently by the Bragg structure. ϖ is the normalized frequency, then the Bragg period,

$$d = \varpi \cdot \frac{2\pi c}{\omega} = \varpi \cdot \lambda,$$

$$d_1 = d \cdot h_1, \qquad d_2 = d \cdot (1 - h_1).$$
 (6)

On substituting Eqs. (1) and (6) into the grating equation, and solving for M,

$$M = \frac{n_{\text{eff}} N \varpi}{\sin \theta} (\sin \alpha + \sin \beta).$$
 (7)

Considering the blazing condition, Eq. (7) then reduces to a simpler form,

$$M = 2n_{\rm eff}N\varpi\cos\phi. \tag{8}$$

In contrast, Eq. (3) can also be derived from the above equation, which indicates that Eq. (8) is the necessary and sufficient criterion for the blazing condition.

Once proper M and N have been selected, a normalized frequency in the photonic bandgap can be obtained. Then, the Bragg period d is determined from Eq. (6), the grating period d by Eq. (1), θ by Eq. (4), and β by Eq. (3).

With the above design method, a perfect matching of diffraction grating condition and Bragg reflection condition is presented. The designed blazing grating based on Bragg mirrors has a high efficiency with large bandwidth. In some cases, the calculated ϖ may lie outside of the photonic bandgap, because M and N must be integers. A small shift of the central wavelength could be used to keep high reflectivity.

LD is used to represent the linear dispersion of the diffraction grating along the Rowland circle with certain change in wavelength $(\Delta \lambda)$. By differentiating the grating equation, LD (μm) can be derived,

$$LD = R_{rc} \cdot \left(\frac{2d\beta}{d\lambda}\right) \Delta \lambda = \frac{2R_{rc}M}{a\cos\beta} \frac{n_g}{n_{\text{eff}}^2} \Delta \lambda$$
$$= \frac{(\sin\alpha + \sin\beta)}{\cos\beta} \frac{2R_{rc}}{\lambda} \frac{n_g}{n_{\text{eff}}} \Delta \lambda, \tag{9}$$

where the incident angle is held constant and $n_g = n_{\rm eff} - \lambda (dn_{\rm eff}/d\lambda)$ is the group index of the slab mode. To reduce the above equation to a simpler form, the term $dn_{\rm eff}/d\lambda$ is negligible, and the group index is substituted by $n_{\rm eff}$. With the assumption of blazing diffraction, i.e., $\alpha - \beta = 2\phi$, we obtain a final expression for the linear dispersion at the blazed wavelength (λ_b) ,

$$LD = \frac{4R_{rc}}{\lambda_b} \frac{\sin \theta \cos \phi}{\cos(\theta - \phi)} \Delta \lambda.$$
 (10)

With a designed linear dispersion required, the radius of the Rowland circle and hence the size of the device can be calculated from Eq. (10). A concave diffraction grating based on circular Bragg mirrors using the above method is constructed, as shown in Fig. 5.

Owing to the reflection resulting from the mode mismatching of the single-mode waveguide (input/output silicon nanowire) and the FPR, an array of tapers is used to connect the single-mode waveguides and the FPR, introducing a low-loss mode convention and wide bandwidth for each wavelength channel.

4. SIMULATIONS AND DISCUSSION

The CDG with circular Bragg mirrors was constructed on SOI waveguides, where a 220-nm-thin silicon layer with refractive index $n_1 = 3.476$ (at $\lambda = 1550$ nm) acts as the core layer on top of a 2- μ m silica buried layer ($n_2 = 1.444$) carried on a silicon substrate, leading to an effective index $n_{\rm eff} = 2.848$ of the slab waveguide. With an incident angle $\phi=2^\circ$, the projected bandgap structure of the Bragg mirror for TE mode was calculated in Fig. 4. The parameters here are chosen as N=2 and M = 5, then ϖ can be calculated from Eq. (8) and has value for $\varpi = 0.4390$ lying in the photonic bandgap. The other parameters used are $\alpha=43^{\circ},\ \theta=41^{\circ}$ and $\beta=39^{\circ},$ thus we have d = 680.5 nm and a = 2074.5 nm from Eqs. (6) and (1). The Bragg mirror contains 12 periods, with an alternation of silica (width d_2) and silicon (width d_1) waveguide. The width ratio varies from 0.56 to 0.62 with an increase of 0.02 to create a broad work band.

An initial computation was performed using finite-difference time-domain (FDTD) solutions software in a two-dimensional (2D) way, with indices $n_{\rm eff}$ and n_2 for the alternating media [20]. The Bragg mirror reached a maximum reflection efficiency of -0.013 dB (99.7%) around the central wavelength over a broad bandwidth about 330 nm at different width ratios, as presented in Fig. 6. It appears that a slight deviation of the etched silica layer have a negligible impact on the performance of the grating facet. Considering the possible etching error in fabrication, the width ratio was selected $h_1 = 0.62$ here.

A 3D simulation of the Bragg mirror with a 220 nm silicon core layer surrounded by silica element was also carried out in the TE polarization mode source, which reveals a slight difference as compared with the 2D result due to the material dispersion. However, the reflection bandwidth is still broad enough, and the scatting losses in the third dimensional are extremely low, i.e., the reflection condition has been satisfied.

The wavelength spacing between output channels is chosen as $\Delta\lambda=10$ nm. An array of 4.5 μ m-wide output waveguides are placed on the Rowland circle with a gap of 1.5 μ m. Then the radius of the Rowland circle can be calculated from Eq. (10), which results in $R_{rc}=275~\mu$ m in this design. The concave grating is simulated by FDTD solutions with a Gaussian source (TE mode) in a 2D fashion, using the effective index $n_{\rm eff}$ previously mentioned. The grating efficiency for the diffraction order was calculated as shown in Fig. 7, without coupling losses into the waveguides. The grating efficiency is

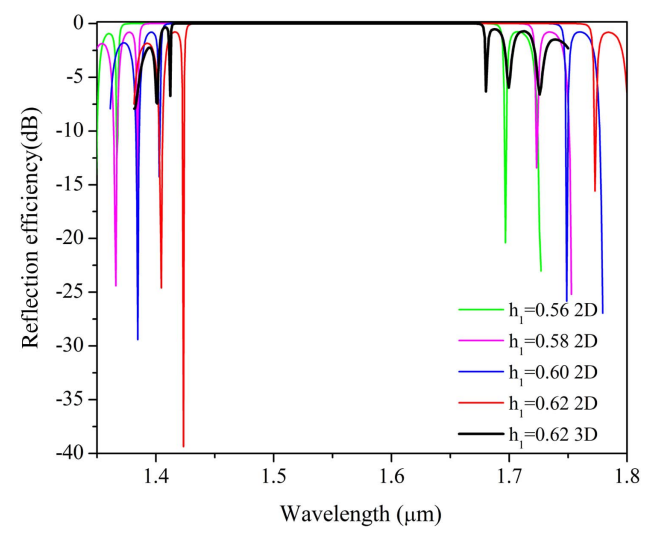


Fig. 6. Reflection spectra of the Bragg mirrors with width ratio from 0.58 to 0.62 in a 2D model, and a 3D simulation at $h_1 = 0.62$ (thick black line).

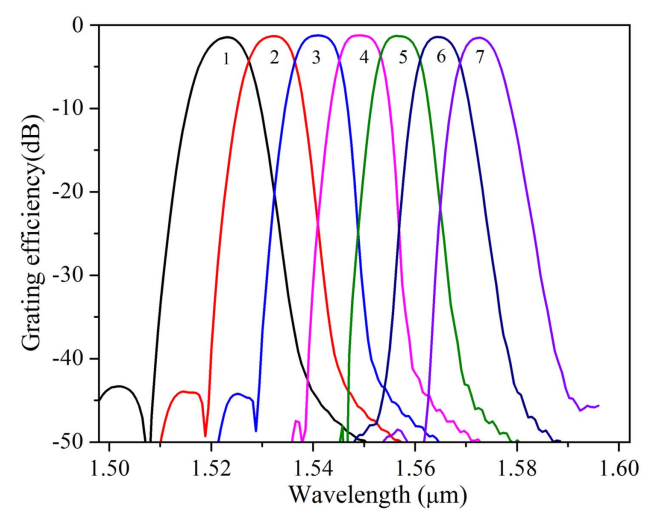


Fig. 7. Output efficiency spectra of the circular Bragg mirrors based diffraction grating with the numbered channels. The power was collected without the output waveguides presented.

-1.30 dB (74.1%) with a channel uniformity of 0.09 dB over the 90 nm spectral range.

The spatial distributions of light at wavelengths of 1.55 and 1.53 μ m were presented in Fig. 8. Note that different light waves are separated in the output channels with a significant space dispersion. For the central wavelength, the major power of the light (75.6%) gets diffracted into the designed order (M=5), i.e., the grating condition is satisfied. However, there is still a little part of light getting diffracted into other orders such as M=4(12.8%). For the light at wavelength of 1.53 μ m, more other diffraction orders are created because the blazing condition is not exactly matched, leading to a degraded grating efficiency.

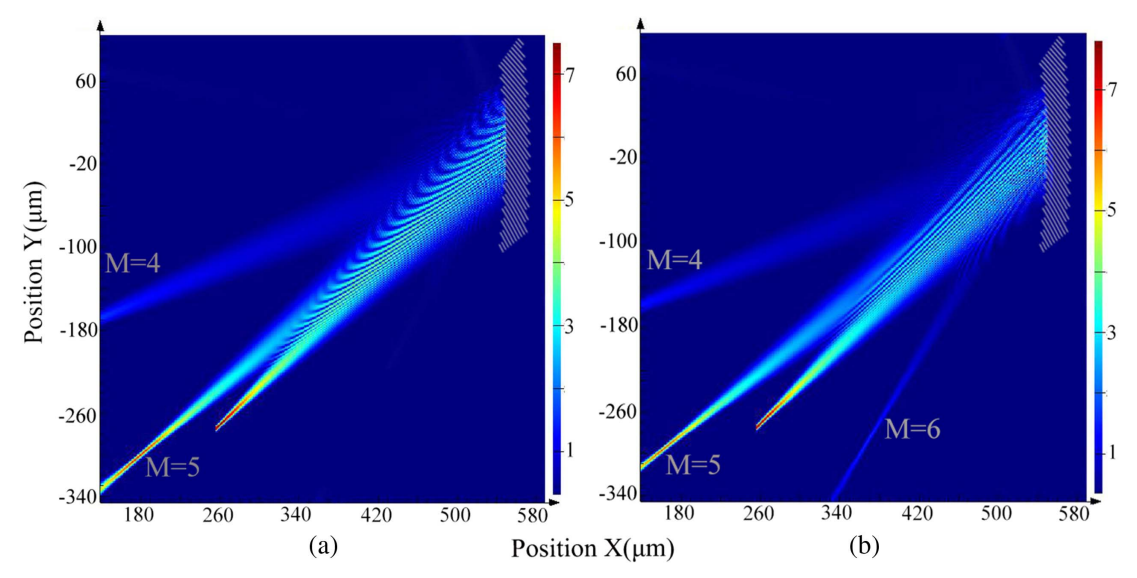


Fig. 8. Spatial distribution of light in the Bragg-CDG for two different wavelengths, (a) 1.55 μ m and (b) 1.53 μ m showing the separation in different channels.

This can be contributed to the presence of the introduced large grating period. The relation between M and a is as follows,

$$M = n_{\text{eff}} \frac{a}{\lambda} (\sin \alpha + \sin \beta) = n_{\text{eff}} N \varpi \frac{\sin \alpha + \sin \beta}{\sin \theta}.$$
 (11)

Then the number of possible diffraction order existed,

$$N_d = M_{\text{max}} - M_{\text{min}} < \frac{2n_{\text{eff}}N\varpi}{\sin\theta},$$
 (12)

which suggests that a low diffraction order as well as insertion loss can be obtained with a small N and ϖ . The blazing condition and the diffraction order codetermine the diffraction efficiency. However, the blazing wavelength may have a slight shift to the central wavelength at a small N and ϖ , because the matching of Bragg condition and grating condition is not perfect (see Fig. 4, N=1, M=2), resulting in a narrow bandwidth.

For a full estimation of the total on-chip loss, the simulation of the grating with access waveguides was also performed using a 2.5D-FDTD tool (VarFDTD Mode solutions). A 30 μm long parabolic taper is used to connect the silicon nanowire and the access waveguide from 0.5 to 4.5 μm . The simulation shows that the taper can achieve a transmission about –0.039 dB (99.1%) at the central wavelength, therefore introducing negligible propagation loss. The output efficiency spectral of the grating with access waveguides was shown in Fig. 9. The grating chip shows an efficiency of –1.72 dB with a channel uniformity 0.34 dB (channels 1–7), and the next-channel crosstalk is about –19.1 dB.

The decrease of the grating efficiency mainly results from the slab propagation loss, and the scattering loss occurred at the junction of output waveguides and the slab region, i.e., a small portion of light is redirected to other channels by the rounded tips of waveguides along the Rowland circle. This scattering of light also leads to a less good crosstalk level. A precise design of the connection boundaries can further

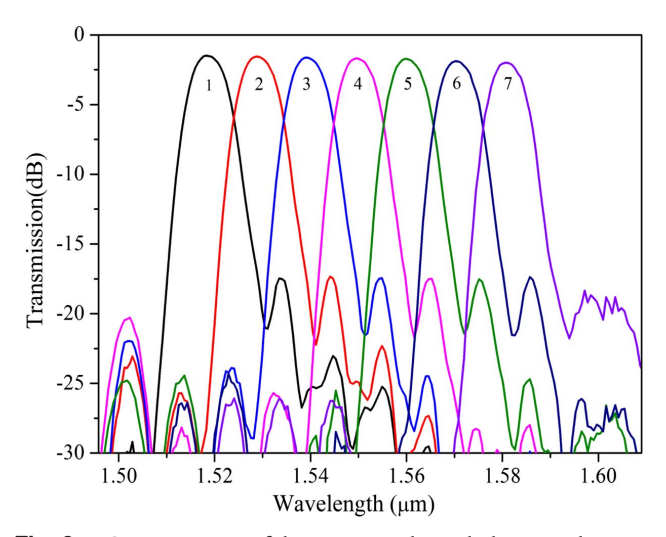


Fig. 9. Output spectra of the grating with parabolic tapers between access waveguides and the FPR.

enhance the grating efficiency and crosstalk. Moreover, the various propagation losses of wavelength introduce a slight shift of the insertion loss of each channel, leading to less good channel uniformity.

5. CONCLUSION

A novel configuration of concave diffraction grating with circular Bragg mirrors has been designed on the SOI platform. With the continuous smooth grating facets, the additional scattering loss from the junction of neighboring grating facets could be effectively suppressed. Moreover, based on one-dimensional photonic crystal bandgap theory, the necessary and sufficient criterion for high grating efficiency has been derived from a

perfect matching of Bragg condition and grating condition. A high order diffraction grating has been designed. The simulation of grating with access waveguides shows a total insertion loss of –1.72 dB with an accurate channel spacing of 10 nm. Such circular Bragg mirror-based grating could be integrated on a small chip to realize a DWDM system as well as a microspectrometer for efficient detection.

Funding. Key Research and Development Plan Foundation of Jiangsu Province, China; National Natural Science Foundation of China (NSFC) (61890961).

REFERENCES

- X. Pommarede, K. Hassan, P. Billondeau, V. Hugues, P. Grosse, B. Charbonnier, and G. H. Duan, "16 x 100 ghz echelle grating-based wavelength multiplexer on silicon-on-insulator platform," IEEE Photon. Technol. Lett. 29, 493–495 (2017).
- H. Yuanshen, L. Ting, X. Banglian, H. Ruijin, T. Chunxian, L. Jinzhong, L. Baicheng, Z. Dawei, N. Zhengji, and Z. Songlin, "Calculation of the diffraction efficiency on concave gratings based on Fresnel-Kirchhoff's diffraction formula," Appl. Opt. 52, 1110–1116 (2013).
- S. Pathak, M. Vanslembrouck, P. Dumon, D. V. Thourhout, and W. Bogaerts, "Optimized silicon awg with flattened spectral response using an mmi aperture," J. Lightwave Technol. 31, 87–93 (2013).
- M. S. D. Smith and K. A. Mcgreer, "Diffraction gratings utilizing total internal reflection facets in littrow configuration," IEEE Photon. Technol. Lett. 11, 84–86 (2002).
- D. Daoxin, F. Xin, S. Yaocheng, and H. Sailing, "Experimental demonstration of an ultracompact si-nanowire-based reflective arrayedwaveguide grating (de)multiplexer with photonic crystal reflectors," Opt. Lett. 35, 2594–2596 (2010).
- L. Chun-Ting, "400-channel 25-ghz-spacing soi-based planar waveguide demultiplexer employing a concave grating across c-and I-bands," Opt. Express 18, 6108–6115 (2010).
- R. Adar, C. H. Henry, C. Dragone, R. C. Kistler, and M. A. Milbrodt, "Broad band array multiplexers made with silica waveguides on silicon," J. Lightwave Technol. 11, 212–219 (1993).
- S. Janz, A. Balakrishnan, S. Charbonneau, P. Cheben, M. Cloutier,
 A. Delage, K. Dossou, L. Erickson, M. Gao, and P. A. Krug,

- "Planar waveguide echelle gratings in silica-on-silicon," IEEE Photon. Technol. Lett. **16**, 503–505 (2004).
- K. Jia, W. Wang, Y. Tang, Y. Yang, J. Yang, X. Jiang, Y. Wu, M. Wang, and Y. Wang, "Silicon-on-insulator-based optical demultiplexer employing turning-mirror-integrated arrayed-waveguide grating," IEEE Photon. Technol. Lett. 17, 378–380 (2005).
- C. Sciancalepore, L. J. Richard, J. A. Dallery, S. Pauliac, K. Hassan, J. Harduin, H. Duprez, U. Weidenmueller, D. F. G. Gallagher, and S. Menezo, "Low-crosstalk fabrication-insensitive echelle grating demultiplexers on silicon-on-insulator," IEEE Photon. Technol. Lett. 27, 494–497 (2015).
- W. Bogaerts, S. K. Selvaraja, P. Dumon, J. Brouckaert, K. D. Vos, D. V. Thourhout, and R. Baets, "Silicon-on-insulator spectral filters fabricated with CMOS technology," IEEE J. Sel. Top. Quantum Electron. 16, 33–44 (2014).
- S. Pathak, P. Dumon, D. V. Thourhout, and W. Bogaerts, "Comparison of awgs and echelle gratings for wavelength division multiplexing on silicon-on-insulator," IEEE Photon. J. 6, 1–9 (2014).
- M. K. Smit and C. V. Dam, "Phasar-based wdm-devices: Principles, design and applications," IEEE J. Sel. Top. Quantum Electron. 2, 236–250 (2002).
- P. Pottier and M. Packirisamy, "Mono-order high-efficiency dielectric concave diffraction grating," J. Lightwave Technol. 30, 2922–2928 (2012).
- J. N. Winn, Y. Fink, S. Fan, and J. D. Joannopoulos, "Omnidirectional reflection from a one-dimensional photonic crystal," Opt. Lett. 23, 1573–1575 (1998).
- Y. Fink, J. N. Winn, S. Fan, C. Chen, J. Michel, J. D. Joannopoulos, and E. L. Thomas, "A dielectric omnidirectional reflector," Science 282, 1679–1682 (1998).
- J. Brouckaert, W. Bogaerts, S. Selvaraja, P. Dumon, R. Baets, and D. V. Thourhout, "Planar concave grating demultiplexer with high reflective Bragg reflector facets," IEEE Photon. Technol. Lett. 20, 309–311 (2008).
- B. Du, J. Zhu, Y. Mao, B. Li, Y. Zhang, and X. Hou, "A design method based on photonic crystal theory for Bragg concave diffraction grating," Opt. Commun. 385, 92–96 (2017).
- Y. Mao, J. Zhu, B. Du, and X. Hou, "Design and analysis of concave diffraction grating with one-dimensional photonic bandgap structure," Opt. Quantum Electron. 49, 263 (2017).
- P. Pottier, M. J. Strain, and M. Packirisamy, "Integrated microspectrometer with elliptical Bragg mirror enhanced diffraction grating on silicon on insulator," ACS Photon. 1, 430–436 (2014).